

Seismic images of the megathrust rupture during the 25th October 2010 Pagai earthquake, SW Sumatra: Frontal rupture and large tsunami

Satish C. Singh, Nugroho Hananto, Maruf Mukti, Haryadi Permana, Yusuf Djajadihardja, Heri Harjono

▶ **To cite this version:**

Satish C. Singh, Nugroho Hananto, Maruf Mukti, Haryadi Permana, Yusuf Djajadihardja, et al.. Seismic images of the megathrust rupture during the 25th October 2010 Pagai earthquake, SW Sumatra: Frontal rupture and large tsunami. Geophysical Research Letters, 2011, 38, 10.1029/2011GL048935 . insu-03606457

HAL Id: insu-03606457
https://insu.hal.science/insu-03606457

Submitted on 12 Mar 2022

HAL is a multi-disciplinary open access archive for the deposit and dissemination of scientific research documents, whether they are published or not. The documents may come from teaching and research institutions in France or abroad, or from public or private research centers.

L'archive ouverte pluridisciplinaire **HAL**, est destinée au dépôt et à la diffusion de documents scientifiques de niveau recherche, publiés ou non, émanant des établissements d'enseignement et de recherche français ou étrangers, des laboratoires publics ou privés.

Copyright

Seismic images of the megathrust rupture during the 25th October 2010 Pagai earthquake, SW Sumatra: Frontal rupture and large tsunami

Satish C. Singh,[1] Nugroho Hananto,[1] Maruf Mukti,[1] Haryadi Permana,[2] Yusuf Djajadihardja,[3] and Heri Harjono[2]

Received 19 July 2011; revised 21 July 2011; accepted 21 July 2011; published 26 August 2011.

[1] The Mentawai segment of the Sumatra subduction zone is locked and likely to produce a large earthquake in the near future. A part of this locked zone ruptured on 12 September 2007 producing twin earthquakes of Mw = 8.5 and 7.9. Recently, a third earthquake of Mw = 7.8 occurred on the 25th October 2010, SW of Pagai Island, Sumatra. The earthquake generated an unexpected very large tsunami on Pagai Islands with run-up height of up to 8 m. Here we present seismic reflection and bathymetry images from the 2010 epicentral region acquired before the earthquake. We find that the frontal thrust is the main active fault in this region and might have ruptured up to the seafloor at 6 km water depth uplifting the water column and producing a large tsunami. Furthermore, finite fault models indicate that this earthquake ruptured the frontal section of the subduction zone, which is generally believed to slip aseismically and be incapable of producing large earthquakes. The presence of aftershocks near the subduction front further confirms that the frontal section of the subduction zone is not aseismic. If the rest of the Mentawai locked zone ruptures the frontal section of the subduction zone during a megathrust, then the resulting tsunami in the Indian Ocean could be devastating. **Citation:** Singh, S. C., N. Hananto, M. Mukti, H. Permana, Y. Djajadihardja, and H. Harjono (2011), Seismic images of the megathrust rupture during the 25th October 2010 Pagai earthquake, SW Sumatra: Frontal rupture and large tsunami, *Geophys. Res. Lett.*, *38*, L16313, doi:10.1029/2011GL048935.

1. Introduction

[2] The Sumatra subduction zone is the most seismically active region on earth. The recent activity initiated with the 2004 Boxing Day great Sumatra-Andaman earthquake of Mw = 9.3 that produced a destructive tsunami in the Indian Ocean with a death toll of >230,000. It ruptured over 1300 km of the plate boundary from northern Sumatra near Simeulue Island to the Andaman Islands [*Ammon et al.*, 2005]. The second great earthquake of Mw = 8.6 occurred three months later on March 28, 2005 about 150 km further southeast near Nias Island breaking 350 km of the plate boundary [*Briggs et al.*, 2006]. After a quiescence of about three years, another great earthquake of Mw = 8.5 occurred on September 12, 2007 about 1300 km from the Boxing Day event near Bengkulu, offshore western Sumatra. This was followed by a second earthquake of Mw = 7.9 twelve hours later, leaving a gap of about 600 km between the 2005 and 2007 earthquakes. The focal depth, the fault plane solution and rupture modelling studies suggest that the second earthquake ruptured the down-dip limit of the main event (Figure 1a) [*Konca et al.*, 2008]. Another Mw = 7.8 earthquake occurred in 2009, but the great depth (~80 km) and the focal mechanism suggest that it occurred within the subducting oceanic plate [*McCloskey et al.*, 2010].

[3] On October 25, 2010, another earthquake of Mw = 7.8 occurred SW of Pagai Island. This earthquake was unusual in the sense that it produced a very large localized tsunami with run up heights reaching up to 3–8 m on the SW coast of Pagai Island killing more than 500 people, injuring >11000 people and destroying over 25000 homes. Apart from the large tsunami for the 2004 earthquake with run-up heights reaching up to 30 m, the tsunamis from the 2005 and 2007 earthquakes were of small to moderate sizes with run-up heights reaching up to 4 m [*Geist et al.*, 2008 and 0.5 m [*Lorito et al.*, 2008], respectively. The United States Geological Survey (USGS) reported the hypocenter at 40 km SW of Pagai Island, ~30 km NE of the subduction front, at a depth of about 20 km, with a dip of 12°. On the other hand, the Global Centroid Moment Tensor (GCMT) location lies beneath the oceanic crust, at ~40 km SW of the subduction front at 12 km depth; it is not possible to have a megathrust earthquake over the oceanic plate. The hypocenter using a local network by the Indonesian agency (BMKG) lies between the two at 20 km NE of the subduction front at 10 km depth (Figure 1b).

[4] In the past, two great earthquakes have occurred in this region: the 1797 earthquake of Mw ~ 8.4 and the 1833 earthquake of Mw ~ 9 [*Prawirodirdjo et al.*, 2000]. The 1797 earthquake produced a devastating tsunami in Padang with a run up height of more than 10 m. Using GPS and coral geodetic data, *Chlieh et al.* [2008] suggested that a slip of up to 8 m might have accumulated since these two great earthquakes (Figure 1a), and this region is fully locked and may produce great earthquakes in the near future. The 2007 twin earthquake ruptured only a part of the locked zone [*Konca et al.*, 2008]. Although the forward modeling study of *Chlieh et al.* [2008] suggests that the plate coupling extends up to the subduction front in this region, no earthquake was expected near the front due to aseismic behavior of sediment-basalt interface [*Wang*, 1980]. Therefore, the occurrence of the Mw = 7.8 earthquake on October 25, 2010

[1] Laboratoire de Géosciences Marines, Institut de Physique du Globe de Paris, Paris, France.
[2] Research Center for Geotechnology, LIPI, West Java, Indonesia.
[3] Agency for the Assessment and Application of Technology, Jakarta, Indonesia.

Copyright 2011 by the American Geophysical Union.
0094-8276/11/2011GL048935

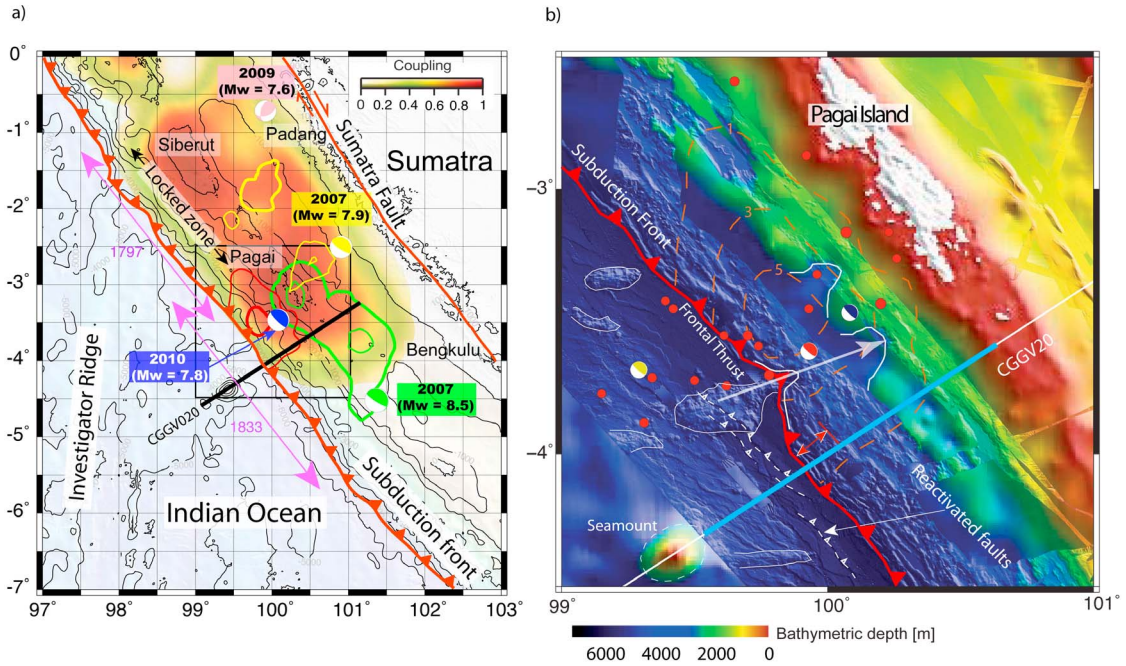


Figure 1. (a) Mentawai segment of the Sumatra subduction zone. The colored beach balls indicate the USGS epicentral locations and fault plane solutions of four earthquakes (2007, 2007, 2009, 2010) in the Mentawai region since 2007. Mw is magnitude. Color contours are 1 m (thin) and 5 m (thick) slip during the megathrust earthquakes: Red for Shao and Ji (unpublished manuscript, 2010), Yellow and Green for 2007 [*Konca et al.*, 2008]. Red and yellow overlay is the plate coupling before these earthquakes from *Chlieh et al.* [2008]. Black line indicates the position of the seismic profile CGGV020. The purple double arrows indicate the 1797 and 1833 earthquake rupture zone [*Chlieh et al.*, 2008]. Thin black rectangle marks the position of image shown in Figure 1b. (b) Yellow beach ball: GCMT location, Blue beach ball: USGS (NEIC) location, Red beach ball: BMKG location. Red curves indicate the slip at 2 m intervals. Thin white curve bounds high bathymetric features on the oceanic plate and low bathymetry anomalies (furrows) on the accretionary prism. Dashed white curves indicate faults on the oceanic crust. Thick red curve with triangles is the frontal thrust. Light white arrow indicates alignment of the bathymetric feature on the oceanic plate with furrows. Red double arrow indicates the offset at the subduction front. Blue line indicates the portion of seismic profile CGGV020 shown in Figures 2a and 3a.

was a surprise, and the large tsunami was even more surprising. In this paper, we present seismic reflection and bathymetric data from the epicenter region of the 2010 earthquake and discuss the cause of the unusual nature of this earthquake and its possible consequences on future earthquakes and tsunamis in the Mentawai region.

2. Seismological Observations

[5] Soon after the earthquake, G. Shao and C. Ji (Preliminary result of the October 25, 2010 Mw 7.85 Sumatra earthquake, 2010, available at http://www.geol.ucsb.edu/faculty/ji/big_earthquakes/2010/10/25/sumatra_update.html, hereinafter referred to as Shao and Ji, unpublished manuscript, 2010) carried out waveform modelling to determine a finite fault model for the 2010 earthquake. They used the global seismic network (GSN) broadband waveforms (26 teleseismic P-wave, 18 SH-wave, and 40 long period surface wave) from the IRIS DMC. They used the USGS epicenter location and the NEIC fault plane solution. However, their model required a depth of 12 km and a dip of 7.5°, less than that reported by USGS. Shao and Ji (unpublished manuscript, 2010) found that the rupture had a maximum slip of 5.5 m concentrated near the subduction front up-dip of the epicenter (Figure 1b). These results might explain why the GCMT location lies on the oceanic plate instead of at the plate interface. The aftershocks data for the first two weeks after the earthquake determined by BMKG (Figure 1b) indicate that these events also lie NW of the epicenter and extend from SW of Pagai Island to more than 50 km SW of the subduction front, beyond the GCMT location on the oceanic plate. Two conclusions can be drawn from these observations: (1) the 2010 earthquake ruptured the frontal section of the subduction front, which contradicts the existing model of subduction zone earthquakes that requires the frontal section of the subduction zone to slip aseismically incapable of producing large earthquakes, and (2) the rupture propagated northwestwards parallel to the subduction front requiring a barrier SE of the epicenter.

3. Seismic Reflection Results

[6] In order to study the seismic and tsunami risks from an imminent great earthquake in the Mentawai region, we acquired deep seismic reflection data in 2009. The data was acquired on board the CGGVeritas seismic vessel, the Geowave Champion, towing one 15 km-long streamer, the largest streamer ever used, and two 6 km-long streamers in the over

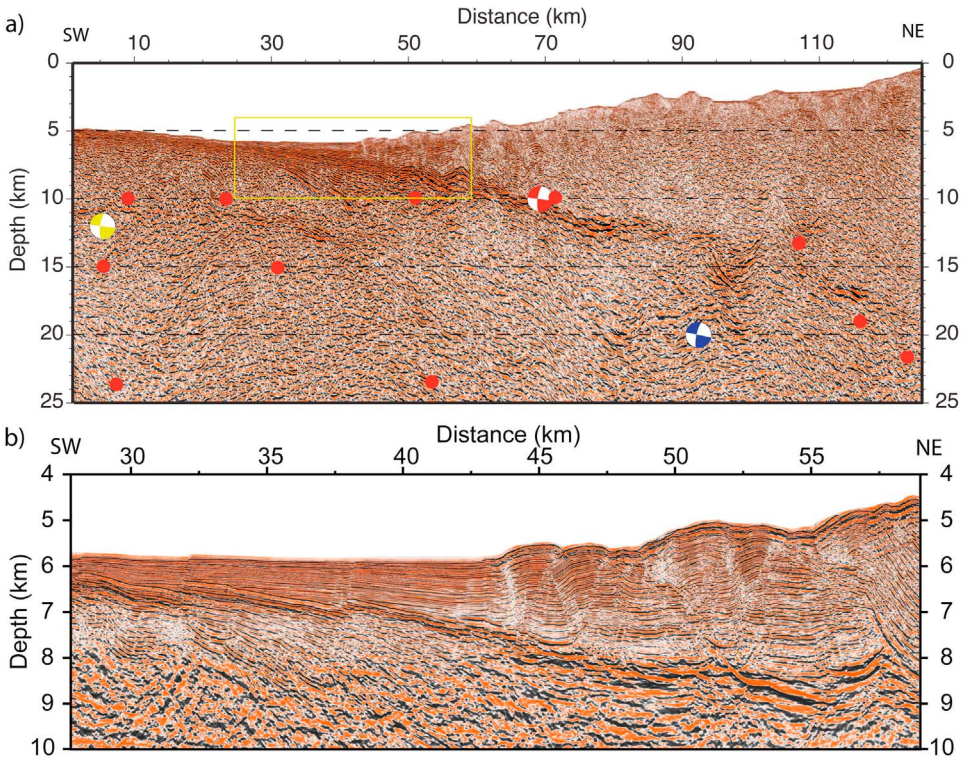


Figure 2. (a) Depth converted non-interpreted seismic reflection image along profile CGGV020. Beach balls indicate the projection of the hypocenters and GCMT locations of the 2010 Pagai earthquake on the profile. Red circles indicate the projected location of the aftershocks. Yellow rectangle indicates the portion of the image shown in Figure 2b. Vertical to horizontal scale is 1:2.

and under configuration [*Singh et al.*, 1996; *Singh et al.*, 2009]. The long streamer was towed at 22.5 m water depth, and the two short streamers at 15 m and 7.5 m. The streamer spacing was 50 m. An array of 48 airguns with a total volume of 9600 cubic inch was towed at 15 m water depth providing the very large low-frequency energy source required to image deep targets. The receiver group interval was 12.5 m and the shot interval was 50 m, providing a fold of 300 for the long streamer, enhancing the signal-to-noise ratio significantly, which is essential for deep crustal imaging. The record length was 20 s, which corresponds to a depth of 55–60 km. The vessel speed was 4–4.5 knots.

[7] The data were first processed using conventional processing techniques to enhance low-frequency energy for deep imaging [*Singh et al.*, 2008, 2011]. A combination of Radon multiple removal and surface-related multiple removal techniques was deployed to remove the water bottom multiples. The velocity was determined using a combination of constant velocity analysis technique and prestack time migration velocity analyses. The data was then migrated using a Kirchhoff time migration technique. The interval velocity determined from the stacking velocity was used to convert the seismic image to depth image. In the second stage of processing, the data from three streamers were combined [*Singh et al.*, 1996] and a pre-stack depth migration was performed to obtain high-resolution seismic of the sedimentary strata.

[8] Seismic profile CGGV020 was designed to cross the 2007 earthquake rupture zone, and coincidently traverses the southeast boundary of the 2010 earthquake rupture zone, at 40 km from the epicenter (Figure 1). The depth converted seismic images along a part of the profile are shown in Figures 2a and 3a, which clearly show the top of the subducting oceanic plate and the oceanic Moho down to 25 km depth beneath the accretionary prism. The dip of the plate interface is about 7.5° up-dip of the epicenter, which increases to ~12° at ~110 km distance range towards the down-dip. The sediment thickness increases from a few hundred meters to 1.2 km near the trench, and to 18 km beneath the accretionary prism at ~80 km inwards. The high-resolution pre-stack depth image (Figures 2b, 3b, and 4) on the oceanic plate shows sediments onlapping over the top of oceanic crust. The top of the oceanic crust is marked by a pair of reflectors ~350 m apart; the upper reflector may correspond to the top of the pelagic sediments or the lava flow from the seamount and the lower reflector could be the top of the basaltic crust. There are at least three seaward dipping normal faults over the oceanic plate (NF1, NF2, NF3). These faults offset the crustal reflectors by 300–400 m, and seem to also offset the Moho, and may have been formed during the bending of the plate in the outer arc rise. Both bathymetry and seismic image suggest that these faults are still active. However, a detailed analysis of the seismic image shows these faults are also sites of re-activated thrust faulting. We also observe a band of landward dipping reflective zone in the oceanic crust with increasing thickness towards the subduction front, possibly resulting from internal shortening within the oceanic crust.

[9] Near the subduction front (at 42.5 km in Figure 3b), a clear landward dipping thrust fault is imaged, which does not have any bathymetric expression on the seafloor, and might be the seaward propagating branch of the megathrust.

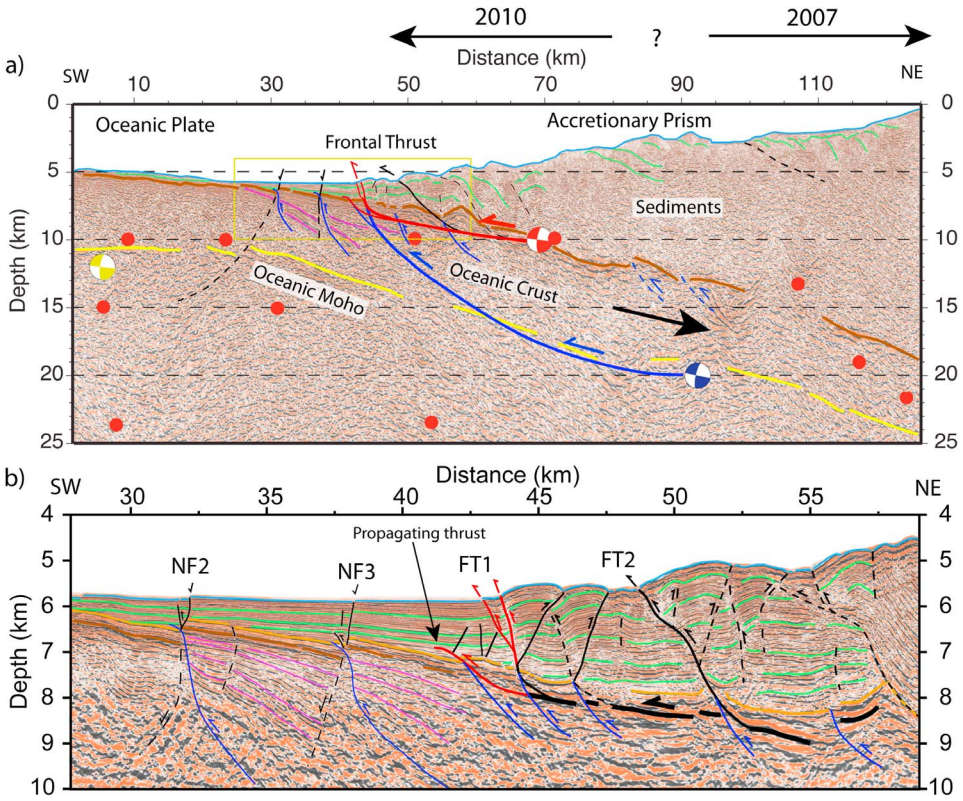


Figure 3. (a) Depth converted interpreted seismic reflection image along profile CGGV020. Beach balls indicate the projection of the hypocenters and GCMT locations of the 2010 Pagai earthquake on the profile. Green curves: sediments; Brown curves: Top of the oceanic crust; Pink curves: structures in the oceanic crust; Yellow: Oceanic Moho, Black Faults. Blue: thrust faults in the oceanic crust. Red circles indicate the projected location of the aftershocks. Yellow rectangle indicates the portion of the image shown in Figure 3b. Thick red curve: Megathrust at top of oceanic crust: Thick blue curve: Megathrust in oceanic plate. Thin blue curves indicate active (solid) and inactive (dashed) thrust in the crust. Thin black curves represent active (solid) and inactive faults. The 2007 and 2010 earthquake rupture zones are marked by the black arrows. (b) Blow-up of high-resolution seismic image marked by yellow rectangle in Figure 3a. NF: Normal faults, FT: Frontal thrusts. Vertical to horizontal scale is 1:2.

At the subduction front, there is a pair of steeply dipping thrust faults (FT1) that seem to cut through the top of the oceanic crust. The seaward branch of FT1 has a fault scarp of ~40 m, and might be the main site of the seafloor rupture during the 2010 earthquake. A seaward dipping conjugate fault intersects FT1 just above the basement and bounds a 2.5-km wide first frontal fold. A second active frontal thrust (FT2) is ~7 km from the front. The high-resolution seismic image clearly shows that the frontal 30 km of the accretionary prism consists of a 3-5 km-wide folds bounded by a pair of conjugate faults. The steeply landward-dipping faults seem to originate at the oceanic crust whereas the seaward-dipping conjugate faults merge the landward-dipping faults within accretionary sediments, suggesting that the main slip occurs along the landward thrust faults.

[10] The top of the oceanic crust is not flat but has undulations, with heights up to 1.5 km (Figure 2). Although we cannot rule out the possible role of seafloor topography and velocity pull-up, some of these features seem to be real. On the oceanic plate just SW of the subduction front, bathymetric data clearly show linear as well as circular (seamount) bathymetric features, and it is possible that the images observed on the seismic profile are subducted features on the top of the oceanic crust. On the other hand, they could result from the re-activation of thrusts within the oceanic crust as observed on the oceanic plate (Figures 3 and 4).

4. Discussion and Conclusions

[11] It is clear from the seismic and bathymetric images that the frontal thrusts (FT1 and FT2) are the most active thrusts and there is a 40 m fault scarp at FT1. It is likely that the main megathrust rupture arrived near FT1 causing an uplift of water column near the front at 6 km water depth and producing the mysterious large tsunami. The projections of the 2010 hypocenters on the seismic profile suggest that the USGS hypocenter lies in the subducting oceanic plate, around the oceanic Moho, whereas the GCMT location is on the Indo-Australian plate near the ocean Moho. On the other hand the hypocenter determined by the local network lies on the plate interface at 10 km depth (Figure 2a). Although these locations might have large uncertainty, they can be used to gain some insight on the link between seismic and bathymetric images and the 2010 earthquake megathrust rupture.

[12] Based on deep seismic images in the 2004 great Andaman-Sumatra earthquake region, *Singh et al.* [2008]

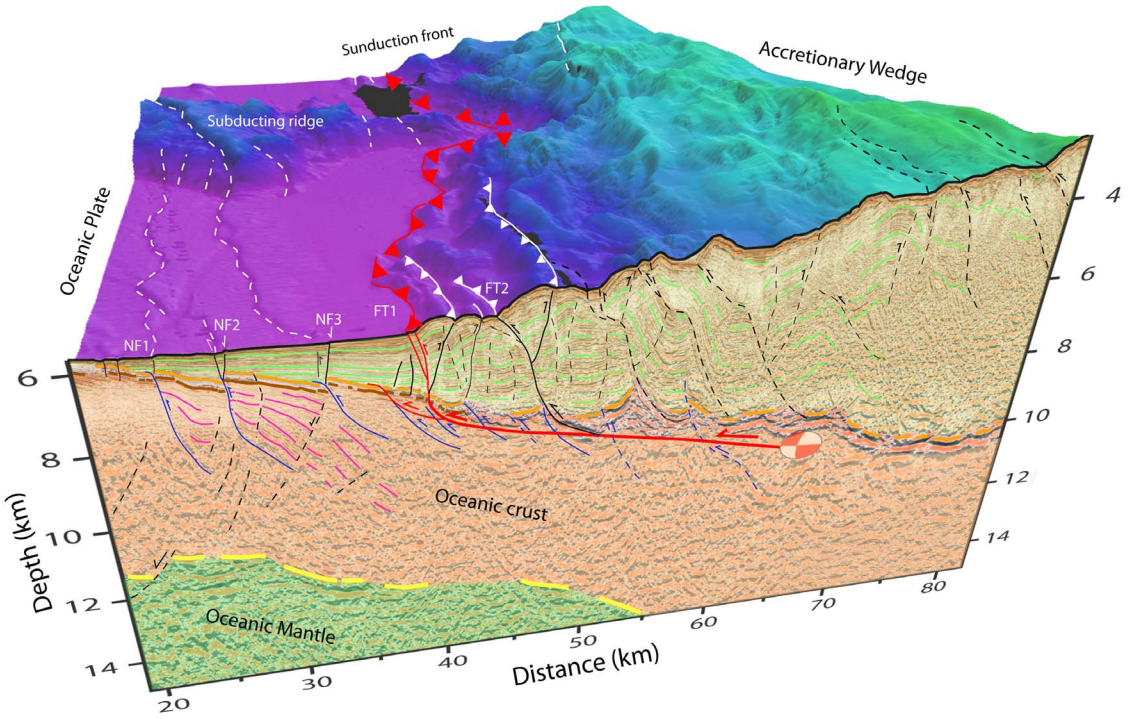


Figure 4. Three dimensional block diagram showing seismic reflection image and corresponding bathymetry. Red beach ball indicates the BMKG hypocenter projection on the seismic profile. Dashed white lines on the seafloor are faults on the oceanic plate, thick white lines are active thrust faults and black dashed lines are in-active faults. Red lines indicate the position of preferred megathrust rupture. Thin solid black lines are active faults and thin dashed lines are in-active faults. Blue lines indicate active thrusts and dashed blue lines in-active thrusts in the oceanic crust. Brown lines marked the top of basaltic crust and yellow oceanic Moho. Pink lines are the crustal reflectivity. Green lines are sediments and orange lines are base of the sediments.

suggested that the 2004 earthquake rupture might have been in the oceanic plate and might have arrived at the subduction front, leading to a large tsunami. The presence of the re-activated thrust in the oceanic crust near the subduction front on seismic profile CGGV020 and the deep hypocenter near the oceanic Moho determined by USGS both support this hypothesis. The finite fault model of G. Hayes (Finite fault model: Results of the October 25, 2010 Mw 7.7 southern Sumatra earthquake, 2010 available at http://earthquake.usgs.gov/earthquakes/eqinthenews/2010/usa00043nx/finite_fault.php) has a peak in the slip at 14 to 18 km depths, supporting the idea of the mantle rupture. The presence of the frontal thrust in the oceanic plate would increase the upper limit of the locked zone farther up-dip, including up to the subduction front and the seafloor. Seismic coupling in oceanic crustal and mantle rocks, which fail brittlely, ought to be stronger than between accreted sediments and oceanic basalts [*Kohlstedt et al.*, 1995]. Figure 3a shows the possible location of rupture plane if the megathrust was in the oceanic plate.

[13] On the other hand, if the hypocenter lies at the plate interface as suggested by the local hypocenter location, the rupture should have arrived at the subduction front along the frontal thrust, uplifting the water column and producing a large tsunami (Figure 3a). However, this would require locking of the frontal section at the sediment/basalt interface, which is supposed to slip aseismically [*Wang*, 1980; *Moore and Saffer*, 2001]. The upper limit of locked subduction interfaces is usually thought to correspond to temperatures of 150°C [*Wang*, 1980], coinciding with the dehydration transition from clay (stable sliding) to illite-chlorite (stick-slip). The sediment thickness at the subduction front is ~ 1 km and hence it should not be dehydrated due to sediment loading and compaction, and should behave aseismically. However, a subducted bathymetric feature would have a steeper slope on its landward side where the principal stress would be higher leading to compaction and dehydration, which is likely to increase the coupling coefficient. Furthermore, the change in the dip of the plate interface due to bathymetric features increases the stress on the steep side, creating asperities in the frontal section [*Scholz and Small*, 1997; *Bilek et al.*, 2003]. Bathymetry data show that there are a few small-scale bathymetric features on the oceanic plate, suggesting the possibility of subducted features producing the asperities. However, several authors have argued that the presence of subducted features lead to weak coupling [*Cummins et al.*, 2002; *Mochizuki et al.*, 2008]. Another possibility is that the re-activated thrusts in the oceanic crust can create a saw-tooth morphology at the top of the oceanic crust, which could enhance the coupling between compacted sediments above the saw-toothed oceanic crust (Figures 3 and 4). Since it would be difficult to propagate the megathrust rupture above the saw-toothed oceanic crust, the megathrust rupture might lie in the oceanic crust (Figure 4) or in the oceanic mantle (Figure 3) [*Singh et al.*, 2008]. The presence of the re-activated thrusts and complex oceanic crust interface in Figures 3 and 4 support this hypothesis.

[14] The recent 2011 Tohoku earthquake was an exceptional megathrust earthquake that not only ruptured up to the subduction front but the maximum slip (~50 m) was also near the front [*Ide et al.*, 2011; S. Kodaira, personal communication, 2011]. Furthermore, the large tsunami seems to have been associated with the large slip near the subduction front. We believe that the large tsunami during the 2004 Aceh earthquake was also due to the frontal rupture [*Singh et al.*, 2008]. The 2005 Nias earthquake did not rupture up to the front, and hence did not produce a large tsunami, but it did induce stress that led to aseismic slip within 11 months of the earthquake [*Hsu et al.*, 2006], which suggests that there could be lateral variation in velocity strengthening in the frontal region. On the other hand, the 1907 Simeulue (Mw = 7.8) produced a devastating tsunami, and seems to have ruptured the frontal section of the subduction zone [*Kanamori et al.*, 2010], similar to the 2010 Pagai earthquake.

[15] Recently, *Singh et al.* [2011] have suggested that a subducted seamount leads to bathymetric depression in the wake of the seamount, and creates a weakly coupled zone along its passage, which can act as a barrier for rupture propagation. On the bathymetry data, we do observe a nearly E-W linear bathymetric feature 15 km wide and 1 km high at the subduction front which has produced a furrow in the bathymetry at the subduction front and there is an offset of ~10 km in the subduction front on either side of the furrow. Further up on the accetionary prism, there is another low bathymetric anomaly aligned with this feature. Aftershocks and finite fault models (Figure 1) suggest that the rupture propagated northwestwards parallel to the subduction front only. Therefore, it is possible that the 2010 rupture was stopped due to a weakly coupled zone in the south created by a subducted feature.

[16] The 2010 earthquake in this region was unusual as it ruptured only the frontal section, assumed to be aseismic, and initiated at the up-dip limit of the 2007 earthquake (Figures 1 and 3). The rupturing of the frontal section would go unnoticed during deep megathrust earthquakes as seismological and geodetic data are insensitive to shallow seaward portion of the subduction zone. Despite four earthquakes in the Mentawai region, a 600 km × 150 km section of the plate interface is still fully locked. If the frontal section of the locked zone ruptures in the future during a megathrust earthquake, as was probably the case during the 2004 and 2010 earthquakes, then the resulting earthquake and the subsequent tsunami could be devastating, particularly to the Padang and Mentawai Island regions. Therefore, it is urgent to set up an appropriate risk mitigation system prior to another disastrous tsunami in the Indian Ocean.

[17] **Acknowledgments.** We would like to thank the Chairman and CEO of CGGVeritas for funding the data acquisition and processing. We would like to thank Chen Ji for providing the finite fault model. We would also like to thank Kelly Wiseman for thorough review of the paper and Robin Lacassin for his help in interpreting the high-resolution seismic reflection data. Institut de Physique du Globe de Paris contribution 3206.

References

Ammon, C. J., et al. (2005), Rupture process of the 2004 Sumatra-Andaman earthquake, *Science*, *308*, 1133–1139, doi:10.1126/science.1112260.

Bilek, S., S. Y. Schwartz, and H. R. DeShon (2003), Control of seafloor roughness on earthquake rupture behavior, *Geology*, *31*, 455–458, doi:10.1130/0091-7613(2003)031<0455:COSROE>2.0.CO;2.

Briggs, R. W., et al. (2006), Deformation and slip along the Sunda megathrust in the great 2005 Nias-Simeulue earthquake, *Science*, *311*, 1897–1901, doi:10.1126/science.1122602.

Chlieh, M., J.-P. Avouac, K. Sieh, D. H. Natawidjaja, and J. Galetzka (2008), Investigation of interseismic strain accumulation along the Sunda megathrust, offshore Sumatra, *J. Geophys. Res.*, *113*, B05305, doi:10.1029/2007JB004981.

Cummins, P. R., T. Baba, S. Kodaira, and Y. Kaneda (2002), The 1946 Nankai earthquake and segmentation of the Nankai Trough, *Phys. Earth Planet. Inter.*, *132*, 75–87, doi:10.1016/S0031-9201(02)00045-6.

Geist, E. L., S. L. Bilek, D. Arcas, and V. V. Titov (2008), Differences in tsunami generation between the December 26, 2004 and March 28, 2005 Sumatra earthquakes, *Earth Planets Space*, *58*, 185–193.

Hsu, Y., M. Simons, J.-P. Avouac, J. Galetzka, K. Sieh, M. Chlieh, D. Natawidjaja, L. Prawirodirdjo, and Y. Boch (2006), Frictional afterslip following the 2005 Nias-Simeulue earthquake, Sumatra, *Science*, *312*, 1921–1926, doi:10.1126/science.1126960.

Ide, S., A. Baltay, and G. Beroza (2011), Shallow dynamic overshoot and energetic deep rupture in the 2011 Mw 9.0 Tohoku-Oki earthquake, *Science*, doi:10.1126/science.1207020.

Kanamori, H., L. Rivera, and W. H. K. Lee (2010), Historical seismograms for unraveling a mysterious earthquake: The 1907 Sumatra earthquake, *Geophys. J. Int.*, *183*, 358–374, doi:10.1111/j.1365-246X.2010.04731.x.

Kohlstedt, D. L., B. Evans, and S. J. Mackwell (1995), Strength of the lithosphere: constraints imposed by laboratory experiments, *J. Geophys. Res.*, *100*, 17,587–17,602, doi:10.1029/95JB01460.

Konca, A. O., et al. (2008), Partial rupture of a locked patch of the Sumatra megathrust during the 2007 earthquake sequence, *Nature*, *456*, 631–635, doi:10.1038/nature07572.

Lorito, S., F. Romano, A. Piatanesi, and E. Boschi (2008), Source process of the September 12, 2007, M_w 8.4 southern Sumatra earthquake from tsunami tide gauge record inversion, *Geophys. Res. Lett.*, *35*, L02310, doi:10.1029/2007GL032661.

McCloskey, J., D. Lange, F. Tilmann, S. Nalbant, A. Bell, D. Natawidjaja, and A. Rietbrock (2010), The September 2009 Padang earthquake, *Nat. Geosci.*, *3*, 70–71, doi:10.1038/ngeo753.

Mochizuki, K., T. Yamada, M. Shinohara, Y. Yamanaka, and T. Kanazawa (2008), Weak interplate coupling by seamounts and repeating M ~ 7 earthquakes, *Science*, *321*, 1194–1197, doi:10.1126/science.1160250.

Moore, J. C., and D. Saffer (2001), Updip limit of the seismogenic zone beneath the accretionary prism of southwest Japan: An effect of diagenetic to low grade metamorphic processes and increasing effective stress, *Geology*, *29*, 183–186, doi:10.1130/0091-7613(2001)029<0183:ULOTSZ>2.0.CO;2.

Prawirodirdjo, L., Y. Bock, J. F. Genrich, S. S. O. Puntodewo, J. Rais, C. Subarya, and S. Sutisna (2000), One century of tectonic deformation along the Sumatran fault from triangulation and Global Positioning System surveys, *J. Geophys. Res.*, *105*, 28,343–28,361, doi:10.1029/2000JB900150.

Scholz, C. H., and C. Small (1997), The effect of seamount subduction on seismic coupling, *Geology*, *25*, 487–490, doi:10.1130/0091-7613(1997)025<0487:TEOSSO>2.3.CO;2.

Singh, S. C., R. W. Hobbs, and D. B. Snyder (1996), Broad-band receiver response from dual-streamer data and its application in deep reflection seismology, *Geophysics*, *61*, 232–243, doi:10.1190/1.1443944.

Singh, S. C., et al. (2008), Seismic evidence for broken oceanic crust in the 2004 Sumatra earthquake epicentral region, *Nat. Geosci.*, *1*, 777–781, doi:10.1038/ngeo336.

Singh, S. C., S. Midenet, and Y. Djajadihardja (2009), Seismic survey of the locked and unlocked Sumatra subduction zone, *Eos Trans. AGU*, *90*(49), 471, doi:10.1029/2009EO490002.

Singh, S. C., et al. (2011), Aseismic zone and earthquake segmentation associated with a deep subducted seamount, *Nat. Geosci.*, *4*, 308–311, doi:10.1038/ngeo1119.

Wang, C. Y. (1980), Sediment subduction and frictional sliding in subduction zones, *Geology*, *8*, 530–533, doi:10.1130/0091-7613(1980)8<530:SSAFSI>2.0.CO;2.

Y. Djajadihardja, Agency for the Assessment and Application of Technology, BPPT 2nd Building, 19th Floor, Jl. M. H. Thamrin No. 8, Jakarta 10340, Indonesia.

N. Hananto, M. Mukti, and S. C. Singh, Laboratoire de Géosciences Marines, Institut de Physique du Globe de Paris, Paris F-75238, France. (singh@ipgp.fr)

H. Harjono and H. Permana, Research Center for Geotechnology, LIPI, Jl Sangkuriang, Bandung-40135, West Java, Indonesia.